

Robust Sensor Data Fusion in Local Positioning

P. Scherz ^{#1}, K. Pourvoyeur ^{†2}, S. Schuster ^{†3}, G. Stelzhammer ^{*4}, and A. Stelzer ^{†#5}

[#]*Institute for Communications and Information Engineering, Johannes Kepler University*

[†]*Christian Doppler Laboratory for Integrated Radar Sensors, Johannes Kepler University
Altenbergerstraße 69, Linz A-4040, Austria*

{¹p.scherz, ²k.pourvoyeur, ³s.schuster, ⁵a.stelzer}@icie.jku.at

^{*}*ABATEC Electronic Solutions*

Oberregauer Straße 48, Regau A-4844, Austria

⁴stelzhammer@abatec-ag.com

Abstract—This contribution presents a tightly coupled sensor fusion technique in order to enhance the accuracy and dynamics of a local positioning system. Redundant measurements are processed to achieve the most precise pose information (position and attitude) of a highly dynamic maneuvering target. A sigma-point Kalman filter is used for the sensor fusion process where attention has been laid on a robust initialization in order to guarantee reliable functionality of the real-time sensor fusion system. Therefore, an iterative reweighted least squares (IRLS) parameter estimator has been developed. To verify the theoretical results, measurements are taken of a remote controlled buggy.

I. INTRODUCTION

By applying sensor data fusion techniques to local positioning applications numerous benefits become available. Apart from enhancing the tracking dynamics and accuracy, it is possible to extract non-directly measurable quantities, e.g., attitude information. Furthermore, the combination of partially redundant and sometimes even contradictory sensor information is feasible. In addition, the exploitation of inherently good sensor properties and suppression of specific sensor type limitations is possible. Furthermore, it is feasible to fuse different accurate sensor information. These techniques use more available information about the maneuvering object and merge them in order to gather an optimal state estimate. The sensor fusion system becomes less prone to faulty measurements occurring under non-line of sight conditions since more information is available in the overall system. Especially when sensor fault detection techniques are applied, a highly robust local positioning system can be designed.

The following section gives a description of the used local position measurement system LPM. It explains the basic localization principle of the LPM system and gives some insight into the measurement process. Section III describes the sensor hardware and how it is integrated into the LPM system. In Section IV a robust estimator for initialization of the sensor fusion algorithm is presented. The actual sensor fusion algorithm and its estimation results are illustrated in

Section V and Section VI. Finally, Section VII concludes the paper. Table I in the appendix summarizes the used nomenclature.

II. LPM SYSTEM

In this section the basic principles of the LPM system are given. Further details are given on the implemented telemetry channel which is necessary for data fusion purposes.

A. System Concept

The main concept of the LPM system was introduced in [1] and [2]. The basic measurement principle of the LPM system relies on the well-known frequency-modulated continuous-wave (FMCW) principle [3] with a center frequency of 5.8 GHz utilizing a total bandwidth of 150 MHz and an absolute measurement update rate of 1 kHz. The basic arrangement of an LPM system consists of base stations (BSs) surrounding the field of view. A master BS activates a single measurement transponder (MT) by a control telegram. Hence, during each measurement slot only one single MT is activated. A key technology for every positioning system is the synchronization of distributed components [4]. For the LPM the synchronization problem of the BSs is solved by adding an additional reference transponder (RT), which is located on a fixed and known position. Each BS measures the time difference between the signals of the RT and the MT. The preprocessed raw data and possibly additional telemetry data of each BS is transferred via a data transfer network to a master processing unit (MPU) for data fusion purposes. Fig. 1 shows a sketch of a typical LPM arrangement and signal flow.

B. Measurement Equation

In LPM the measured difference frequency Δf_s at BS_s is converted into a pseudorange $\rho_{\text{LPM},s}$ according to

$$\begin{aligned}\rho_{\text{LPM},s} &= c_0 \frac{T_r}{B_r} \Delta f_s \\ &= \|\mathbf{z}_{\text{MT}} - \mathbf{z}_{\text{BS},s}\|_2 - \|\mathbf{z}_{\text{RT}} - \mathbf{z}_{\text{BS},s}\|_2 + w_{\text{osc}}.\end{aligned}\tag{1}$$

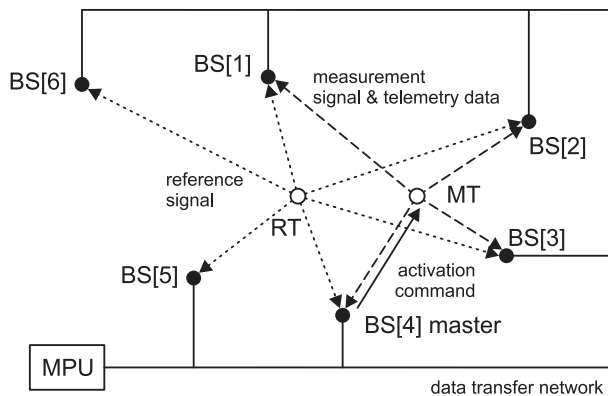


Fig. 1. Typical LPM setup consisting of BSs surrounding the field of view, an MT, as well as an RT. A master BS activates the MT by a trigger telegram and a data transfer network collects the data for further processing at the MPU.

T_r denotes the ramp duration of the FMCW signal ($500 \mu s$), B_r its bandwidth, and c_0 the velocity of propagation of the electromagnetic wave. The measured pseudorange complies to the difference between distance BS-MT and distance BS-RT plus an unknown and drifting measurement offset w_{osc} . The vector coordinates of BS $_s$, MT, and RT are given by $\mathbf{z}_{BS,s}$, \mathbf{z}_{MT} , and \mathbf{z}_{RT} . An unknown measurement offset w_{osc} must be taken into account due to the lack of synchronization between the MT and the RT. The LPM pseudorange ρ_{LPM} given by (1) is similar to the pseudorange ρ_{GPS} used in GPS taking into account the distance $\|\mathbf{z}_{RT} - \mathbf{z}_{BS,s}\|_2$ according to

$$\rho_{GPS,s} \triangleq \rho_{LPM,s} + \|\mathbf{z}_{RT} - \mathbf{z}_{BS,s}\|_2. \quad (2)$$

C. Telemetry Channel

A telemetry channel, introduced in [5], is seamlessly integrated in the transponder hardware. The measurement signals are not affected due to a timing gap within the measurement cycle. Thus the overall measurement update rate remains unchanged high at 1 kHz. At the current development stage a protocol length of 32 bit per transponder activation is implemented. The assignment of these bits is transparent for the user and an error correction can be implemented. Due to the parallel reception of the telemetry data at all BSs a low bit-error rate is obtained.

III. SENSOR UNIT

This section gives a brief description of the sensors and the digital signal processor system, which is integrated into the LPM system in order to provide additional sensor information.

A. Sensor System

Basically, the sensor system consists of a digital signal processing (DSP) board used as a pure computing unit as well as a sensor data capturing, preprocessing, and data management unit based on a field

programmable gate array (FPGA). The whole sensor system is shown in Fig. 2.

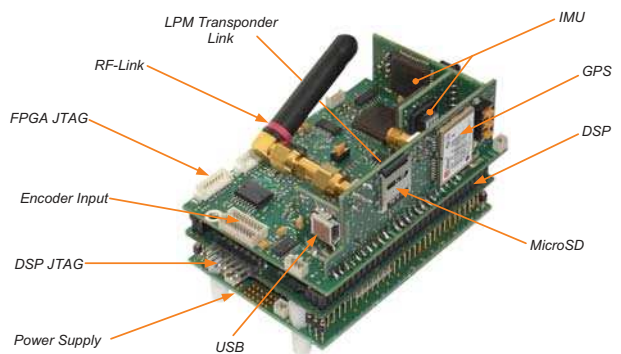


Fig. 2. The FPGA board is mounted at the top of the stack. Underneath, the DSP is placed above the power supply which is attached at the bottom of the stack.

The FPGA comprises an embedded NIOS II soft-core processor which controls the custom developed memory mapped peripherals (MMP). These MMPs are reusable software components performing individual tasks ranging from interfaces to the LPM transponder, I2C, SPI, UART, etc., to more complex functions like controllers for the GPS, encoders, RF-link, mass storage device, and a pulse radar. A more detailed description of the sensor system is given in [6]. The DSP board is intended for on-board sensor fusion as well as guidance and control applications. Nevertheless, the sensor system board can be used without the DSP in a stand-alone mode. Thus the FPGA part of the system, containing all the sensors, may be used as data logger without performing sensor fusion, control or navigational tasks.

B. Sensor Types

For enhanced pose estimation performance several different types of measurements can be combined: pseudoranges of GPS and LPM as well as data from accelerometers, gyroscope sensors, and rotary encoders. Pseudoranges measured by LPM or GPS enable the calculation of an absolute position solution. Although the accuracy of the GPS pseudoranges is significant below the accuracy of the LPM pseudoranges, the worldwide availability of the GPS signal enables a position solution even if the sensor unit is outside the LPM field of coverage. A performance comparison between the GPS and the LPM system is given in [7]. The inertial sensors consisting of tri-axial arranged accelerometers as well as tri-axial arranged gyroscope sensors guarantee a good performance for high dynamic maneuvers but require an absolute fix to compensate a potential bias in the measurements. This is achieved by the pseudoranges of LPM and/or GPS as well as by a rotary encoder. In comparison to inertial sensors, which are affected by bias and scaling errors, a rotary encoder is only influenced

by scaling errors. Therefore, adding an encoder has significant advantages for the basic state estimation performance.

C. Sensor System Integration into LPM

The LPM telemetry channel has not the channel capacity to transfer all available sensor data from the sensor unit to the MPU. Therefore, at every sampling instant where new sensor measurements are available, the sensor system transfers the necessary sensor data only. This data set includes the actual time stamp, rotary encoder, gyroscopes, and accelerometer measurements. Since the sensor and LPM system have different time bases, these data have to be synchronized by the MPU. This is accomplished by using the sensor unit's internal time stamp which is fitted into the LPM time frame. The sensor system's measurement data is broadcasted to the LPM system by only one MT but received by all BSs. This data set is passed to the sensor fusion unit which fuses the available data in postprocessing.

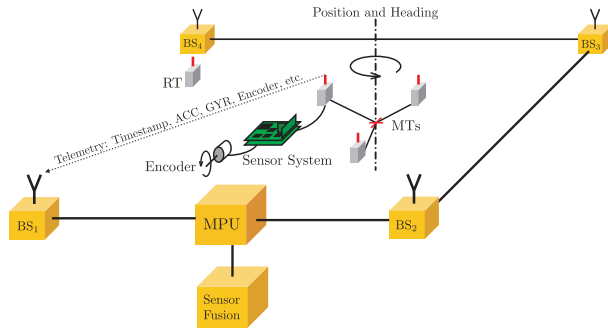


Fig. 3. Example arrangement of four LPM BSs, three MTs, and the sensor system including a rotary encoder which, e.g., is attached to a buggy wheel.

IV. INITIALIZATION

In order to get a coarse position solution of every individual MT, pseudoranges are utilized in the Bancroft algorithm. The Bancroft algorithm, introduced in [8], is a computationally efficient, analytic, non-iterative solution to the GPS absolute positioning problem. In [9] this technique is adapted for the LPM system offering a computationally efficient method for calculating a position solution of the MT. These preliminary MT-positions are used by a robust parameter estimator. Since standard maximum likelihood estimators (MLE) are prone to faulty measurement conditions, which can be caused by synchronization errors, multipath, etc., this method can not ensure to deliver reliable initialization parameters. For this reason a robust parameter estimator, using a 1-norm cost function instead of a 2-norm cost function, has been developed. The results from the standard MLE algorithm (under the Gaussian assumption) are used to derive and initialize the robust estimator.

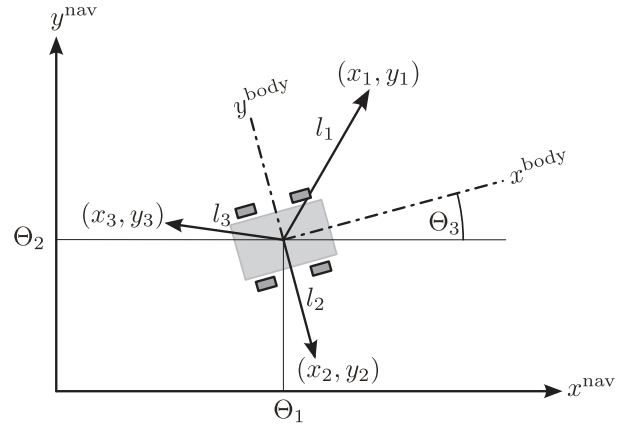


Fig. 4. Sketch of a downscaled vehicle with respect to three vectors pointing to the MTs.

A. MLE Estimator

The following model is used in order to describe a vehicle's position (Θ_1, Θ_2) and its attitude (Θ_3) when M transponders are mounted.

$$\begin{aligned} x_1[n_1] &= \Theta_1 + l_{x,1} \cos(\Theta_3) - l_{y,1} \sin(\Theta_3) + w_{x1}[n_1] \\ y_1[n_1] &= \Theta_2 + l_{x,1} \sin(\Theta_3) + l_{y,1} \cos(\Theta_3) + w_{y1}[n_1] \\ x_2[n_2] &= \Theta_1 + l_{x,2} \cos(\Theta_3) - l_{y,2} \sin(\Theta_3) + w_{x2}[n_2] \\ y_2[n_2] &= \Theta_2 + l_{x,2} \sin(\Theta_3) + l_{y,2} \cos(\Theta_3) + w_{y2}[n_2] \\ &\vdots \\ x_M[n_M] &= \Theta_1 + l_{x,M} \cos(\Theta_3) - l_{y,M} \sin(\Theta_3) + w_{xM}[n_M] \\ y_M[n_M] &= \Theta_2 + l_{x,M} \sin(\Theta_3) + l_{y,M} \cos(\Theta_3) + w_{yM}[n_M] \end{aligned} \quad (3)$$

where $l_{x,1..M}$ and $l_{y,1..M}$ are the x and y offset vector coordinates of the corresponding transponder (in body coordinates) to the tracking point (Θ_1, Θ_2) , n_1, \dots, n_M are the indices of available measurements $(x_1, \dots, x_M, y_1, \dots, y_M)$ for each MT and $w_{x1..M}$ and $w_{y1..M}$ are the additive white Gaussian noise (AWGN) terms. The probability density function for the absolute coordinates of each MT is given by

$$\begin{aligned} p(\mathbf{x}_1; \Theta) &= \frac{1}{2\pi\sigma^{N_1/2}} \exp\left[\frac{-1}{2\sigma^2}(\mathbf{x}_1 - \mathbf{s}_{x1})^T(\mathbf{x}_1 - \mathbf{s}_{x1})\right] \\ p(\mathbf{y}_1; \Theta) &= \frac{1}{2\pi\sigma^{N_1/2}} \exp\left[\frac{-1}{2\sigma^2}(\mathbf{y}_1 - \mathbf{s}_{y1})^T(\mathbf{y}_1 - \mathbf{s}_{y1})\right] \\ p(\mathbf{x}_2; \Theta) &= \frac{1}{2\pi\sigma^{N_2/2}} \exp\left[\frac{-1}{2\sigma^2}(\mathbf{x}_2 - \mathbf{s}_{x2})^T(\mathbf{x}_2 - \mathbf{s}_{x2})\right] \\ &\vdots \end{aligned}$$

with $\mathbf{s}_{x,1}$, $\mathbf{s}_{y,1}$, $\mathbf{s}_{x,2}$, etc. by

$$\begin{aligned} \mathbf{s}_{x,1} &= \Theta_1 + l_{x,1} \cos(\Theta_3) - l_{y,1} \sin(\Theta_3) \\ \mathbf{s}_{y,1} &= \Theta_2 + l_{x,1} \sin(\Theta_3) + l_{y,1} \cos(\Theta_3) \\ &\vdots \end{aligned}$$

When using $\Theta = [\Theta_1 \ \Theta_2 \ \Theta_3]^T$ as parameter vector and assuming the individual probability density functions to be independent, the joint probability density function can be expressed as

$$\begin{aligned} p(\mathbf{x}; \Theta) &= p(\mathbf{x}_1; \Theta)p(\mathbf{y}_1; \Theta) \dots p(\mathbf{x}_M; \Theta)p(\mathbf{y}_M; \Theta) \\ &= \prod_{m=1}^M p(\mathbf{x}_m; \Theta) \cdot p(\mathbf{y}_m; \Theta) \end{aligned} \quad (4)$$

which in turn can be rewritten as

$$p(\mathbf{x}; \Theta) = \frac{1}{2\pi\sigma^N} \exp \left[\frac{-1}{2\sigma^2} \left[\sum_{m=1}^M \mathbf{q}_{x,m}^T \mathbf{q}_{x,m} + \sum_{m=1}^M \mathbf{q}_{y,m}^T \mathbf{q}_{y,m} \right] \right]$$

$$N = N_1 + N_2 + \dots + N_M \quad (5)$$

$$\mathbf{q}_{x,m} = \mathbf{x}_m - \mathbf{s}_{x,m} \quad (6)$$

$$\mathbf{q}_{y,m} = \mathbf{y}_m - \mathbf{s}_{y,m}. \quad (7)$$

The MLE is found by maximizing $p(\mathbf{x}; \Theta)$. Thus taking the derivative of the log-likelihood function and setting equal to zero gives

$$\frac{\partial \ln p(\mathbf{x}; \Theta)}{\partial \Theta} = \frac{\partial}{\partial \Theta} \sum_{m=1}^M (\mathbf{q}_{x,m}^T \mathbf{q}_{x,m} + \mathbf{q}_{y,m}^T \mathbf{q}_{y,m}) = 0. \quad (8)$$

By using a sum equation instead of the vector dot product (8) can be expressed as

$$\frac{\partial \ln p(\mathbf{x}; \Theta)}{\partial \Theta} = \frac{\partial}{\partial \Theta} \sum_{m=1}^M \left[\sum_{n=0}^{N_m-1} q_{x,m}[n]^2 + \sum_{n=0}^{N_m-1} q_{y,m}[n]^2 \right]$$

where again M is the number of MTs in the system and N_m the number of available measurements for each transponder m .

B. Nonlinear Transformation

In order to solve the estimation problem the model equations in (3) are reformulated to a linear problem [10]

$$x_m[n] = \xi_1 + l_{x,m}\xi_3 + l_{y,m}\xi_4 + w_{x,m}[n] \quad (9)$$

$$y_m[n] = \xi_2 + l_{x,m}\xi_4 + l_{y,m}\xi_3 + w_{y,m}[n] \quad (10)$$

$$\xi = [\xi_1 \ \xi_2 \ \xi_3 \ \xi_4]^T =$$

$$\xi = [\Theta_1 \ \Theta_2 \ \cos(\Theta_3) \ \sin(\Theta_3)]^T \quad (11)$$

where (11) is the vector containing the reformulated parameters to estimate and $w_{x,m}$, $w_{y,m}$ are again the noise terms. Hence the model can be written in a linear form

$$\mathbf{x} = \mathbf{H} \xi + \mathbf{w} \quad (12)$$

or explicitly by

$$\begin{bmatrix} x_1[1] \\ y_1[1] \\ \vdots \\ x_1[n_1] \\ y_1[n_1] \\ x_2[1] \\ y_2[1] \\ \vdots \\ x_2[n_2] \\ y_2[n_2] \\ \vdots \\ x_k[1] \\ y_k[1] \\ \vdots \\ x_M[n_M] \\ y_M[n_M] \end{bmatrix} = \begin{bmatrix} 1 & 0 & l_{x,1} & -l_{y,1} \\ 0 & 1 & l_{y,1} & l_{x,1} \\ \vdots & \vdots & \vdots & \vdots \\ 1 & 0 & l_{x,2} & -l_{y,2} \\ 0 & 1 & l_{y,2} & l_{x,2} \\ \vdots & \vdots & \vdots & \vdots \\ 1 & 0 & l_{x,M} & -l_{y,M} \\ 0 & 1 & l_{y,M} & l_{x,M} \end{bmatrix} \begin{bmatrix} \xi_1 \\ \xi_2 \\ \xi_3 \\ \xi_4 \end{bmatrix} + \mathbf{w} \quad (13)$$

where (13) is a rolled-out form of (9) and can be solved straight forwardly by

$$\hat{\xi}_{L2} = (\mathbf{H}^T \mathbf{H})^{-1} \mathbf{H}^T \mathbf{x} \quad (14)$$

which equals a least squares solution. This solution is used to initialize the IRLS algorithm derived in the next subsection.

C. IRLS L1-Regression

To find a 1-norm solution, which is known to be robust against faulty measurements, for the model equations in (3), is more challenging because the derivative of the 1-norm of the residual vector $\mathbf{r} = \mathbf{x} - \mathbf{H}\xi$ in the cost function

$$J(\xi) = \|\mathbf{x} - \mathbf{H}\xi\|_1 = \sum_{i=1}^{2N} |\mathbf{x}_n - \mathbf{H}_i \xi|$$

is not defined at points where $\mathbf{x}_i = \mathbf{H}_i \xi$. Whereas at points where the derivative exists, the 1-norm differentiated with respect to the parameter vector ξ is given by

$$\nabla J(\xi) = \sum_{i=1}^{2N} \mathbf{H}_i \operatorname{sgn}(x_i - \mathbf{H}_i \xi) \quad (15)$$

where \mathbf{H}_i is the i th row vector of \mathbf{H} and $\operatorname{sgn}(\cdot)$ the signum function. In this case ($\xi \in \mathbb{R}^4$) the gradient can be written as

$$\nabla J(\xi) = [j_1 \ j_2 \ j_3 \ j_4]^T, \quad (16)$$

by using the abbreviations j_1 , j_2 , j_3 , and j_4 , and replacing the signum function, where

$$j_u = \frac{\partial J(\xi)}{\partial \xi_u} = \sum_{i=1}^{2N} \mathbf{H}_{i,u} \frac{r_i}{|r_i|} \quad u \in \{1, 2, 3, 4\}. \quad (17)$$

In order to get an estimate for the unknown parameter vector ξ , which is minimizing the 1-norm, (16) is set zero. Defining a diagonal weighting matrix \mathbf{R} with diagonal elements $R_{i,i} = 1/|r_i|$, (17) can be written as

$$\begin{aligned} \nabla J(\xi) &= \mathbf{H}^T \mathbf{R} \mathbf{r} = \mathbf{H}^T \mathbf{R} (\mathbf{x} - \mathbf{H}\xi) = \mathbf{0} \\ \Rightarrow \mathbf{H}^T \mathbf{R} \mathbf{H} \xi &= \mathbf{H}^T \mathbf{R} \mathbf{x}. \end{aligned} \quad (18)$$

In (18) \mathbf{R} depends on the unknown parameter vector ξ , which makes it difficult to solve directly for ξ . A IRLS algorithm [11] iteratively finds the appropriate diagonal weighting elements in \mathbf{R} by using the scheme outlined in (19)-(22):

First $\hat{\xi}$ is initialized with the result of the standard MLE (14)

$$\hat{\xi}_{k,\text{IRLS}} = \hat{\xi}_{\text{L2}}. \quad (19)$$

After that, the new residuals are calculated which are the diagonal elements in \mathbf{R}

$$\hat{\mathbf{r}}_k = \mathbf{x} - \mathbf{H}\hat{\xi}_{k,\text{IRLS}}. \quad (20)$$

In the case that a diagonal absolute weight value is smaller than a predefined value $|r_i|_k < \epsilon$, it is set to $|r_i|_k = \epsilon$, else the IRLS will fail when a residual becomes zero. Then the new weighting matrix \mathbf{R}_k is determined by

$$\hat{\mathbf{R}}_k = \mathbf{R}(\hat{\xi}) = \text{diag} \left(1/|\mathbf{x} - \mathbf{H}\hat{\xi}_{k,\text{IRLS}}| \right) \quad (21)$$

and (18) is solved for the parameter vector

$$\hat{\xi}_{k+1,\text{IRLS}} = (\mathbf{H}^T \hat{\mathbf{R}}_k \mathbf{H})^{-1} \mathbf{H}^T \hat{\mathbf{R}}_k \mathbf{x}. \quad (22)$$

If the difference of the new to the previous estimate falls below a certain threshold level the iteration is canceled. If not, the iteration starts at (20) again.

The position and attitude parameters in vector Θ can now be retrieved again by

$$\Theta_1 = \xi_1 \quad (23)$$

$$\Theta_2 = \xi_2 \quad (24)$$

$$\Rightarrow \frac{\xi_4}{\xi_3} = \tan \Theta_3 \Rightarrow \Theta_3 = \arctan \left(\frac{\xi_4}{\xi_3} \right). \quad (25)$$

These parameters Θ are used to initialize the position and attitude states of the sigma-point Kalman filter. The filter's velocity state is set to zero speed whereas the MT's corresponding measurement offset state is initialized by the outcome of the Bancroft algorithm. Fig. 5 shows a typical initialization difference between a standard MLE and IRLS parameter estimator for artificially generated data (grey dots). Empirical observations have shown that the IRLS estimation matches the real situation well, whereas the results of the standard MLE estimation are inaccurate in the presence of a considerable amount of outliers.

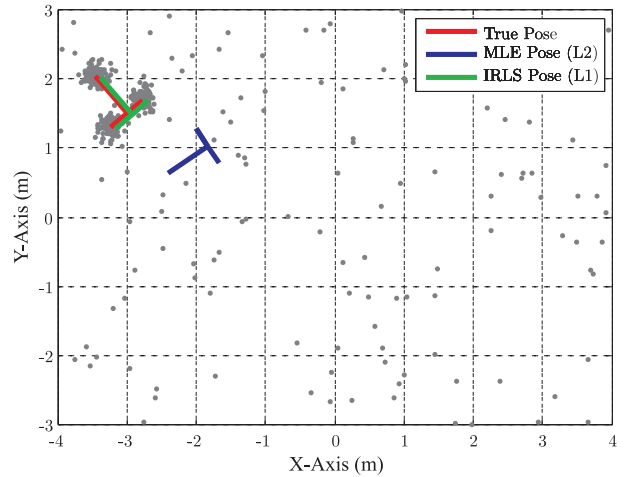


Fig. 5. Three MTs (scatter plot) are combined to estimate an initial position and attitude for the actual sensor fusion algorithm. The artificially generated data correspond to measurements within 0.4 seconds and 40% of outliers. The outliers are uniformly distributed over the field of view.

V. SENSOR FUSION

This section discusses the sigma-point Kalman filter algorithm integrated in the LPM system. A detailed description of sigma-point Kalman filters is given in [12]–[18]. Inertial and incremental encoder measurements, as well as LPM measurements are processed in order to estimate a vehicle's position, velocity, and attitude. It will be shown that the filter's state depends on the number of combined transponders in the system (26). Therefore, the derivative-free filtering technique of sigma-point Kalman filters is very suitable since the process and measurement models have to be adapted online. In the following subsections the process and measurement models, integrated into the sigma-point Kalman filter framework, are discussed followed by a subsection which describes the sensor fusion and a sensor fault detection algorithm.

A. Process Model

The implemented process model can be separated into a linear and nonlinear part, respectively.

$$\mathbf{x}_{k+1} = \mathbf{f}(\mathbf{x}_k) = \begin{bmatrix} \Theta_1 \\ \Theta_2 \\ v \\ \Theta_3 \\ \omega \\ \omega_{\text{bias}} \\ w_{1,\text{osc}} \\ v_{1,\text{osc}} \\ w_{2,\text{osc}} \\ v_{2,\text{osc}} \\ \vdots \\ w_{M,\text{osc}} \\ v_{M,\text{osc}} \end{bmatrix}_{k+1} = \begin{bmatrix} \Theta_1 + v \cos(\Theta_3) T \\ \Theta_2 + v \sin(\Theta_3) T \\ v \\ \psi + \omega T \\ \omega \\ \omega_{\text{bias}} \\ w_{1,\text{osc}} + v_{1,\text{osc}} T \\ v_{1,\text{osc}} \\ w_{2,\text{osc}} + v_{2,\text{osc}} T \\ v_{2,\text{osc}} \\ \vdots \\ w_{M,\text{osc}} + v_{M,\text{osc}} T \\ v_{M,\text{osc}} \end{bmatrix}_k \quad (26)$$

The vehicle's dynamics are described by the nonlinear part, whereas the absolute oscillator offset and oscillator drift velocity of every transponder are represented by the linear part of the process model (26). This process model is integrated into the sigma point Kalman filter framework and is used in order to get a *a priori* state estimate \mathbf{x}_k^- of the position (Θ_1, Θ_2) , velocity (v) , heading (Θ_3) , angular heading velocity (ω) , gyroscope bias (ω_{bias}) , oscillator offsets $(w_{1\dots M, \text{osc}})$, and oscillator offset drifts $(v_{1\dots M, \text{osc}})$. The variable k is reused as time index.

B. Measurement Models

Every millisecond a new LPM measurement is available. The *a priori* state estimate is refined by the update stage using the following measurement models (27), (28) and (29)

$$\tilde{\rho}_{m,s} = \left\| \begin{bmatrix} \Theta_1 \\ \Theta_2 \\ z_p \end{bmatrix} + \mathbf{C}_{\text{bod}}^{\text{nav}}(\Theta_3) \mathbf{l}_m^{\text{bod}} - \begin{bmatrix} BS_{s,x} \\ BS_{s,y} \\ BS_{s,z} \end{bmatrix} \right\|_2 + w_{m,\text{osc}} \quad (27)$$

where $\tilde{\rho}_{m,s}$ is the pseudorange belonging to the transponder m and the base station s . A constant value z_p defines the z-coordinate of the field of view. The direction cosine matrix $\mathbf{C}_{\text{bod}}^{\text{nav}}(\Theta_3)$ transforms the offset coordinate vector $\mathbf{l}_m^{\text{bod}}$ of transponder m from body coordinates into the navigation coordinate system. $BS_{s,x}$, $BS_{s,y}$, and $BS_{s,z}$ are the coordinates of the base station s . Gyroscope measurements $\tilde{\omega}_{\text{gyro}}$ are updated by

$$\tilde{\omega}_{\text{gyro}} = \omega + \omega_{\text{bias}} \quad (28)$$

whereas the angular velocity of the rear left wheel is updated by using

$$\tilde{v}_{\text{wheel}} = \frac{v - \omega d}{R_{\text{wheel}}} \quad (29)$$

where d is the constant distance from the center of the rear axis (tracking point) to the wheel. Experiments have shown that it is acceptable to assume the wheel radius R_{wheel} constant.

C. Sigma Point Kalman Filter Framework

After initializing the state covariance and the state vector with the results from the IRLS, $2(6 + 2M)$ sigma points are calculated by means of a Cholesky factorization. These sigma points are transformed by the process model. From the transformed sigma points the *a priori* state and covariance are determined. Every millisecond new LPM measurements are available and have to pass two plausibility checks. Firstly, the sensor fusion system checks the correctness of the transponder ID as well as the received transponder signal power levels at every BS. Secondly, a χ^2 test is performed. Therefore, the individual innovation of every base station measurement is calculated. For computational reasons this value is computed on the

basis of the gradient vector (instead of using sigma points) in order to generate a measurement vector \mathbf{h}

$$\mathbf{h} = \frac{\partial \tilde{\rho}_{m,s}}{\partial \mathbf{x}} = \begin{bmatrix} \left. \frac{\partial \tilde{\rho}_{m,s}}{\partial \Theta_1} \right|_{\mathbf{x}=\mathbf{x}_k^-} \\ \left. \frac{\partial \tilde{\rho}_{m,s}}{\partial \Theta_2} \right|_{\mathbf{x}=\mathbf{x}_k^-} \\ 0 \\ \left. \frac{\partial \tilde{\rho}_{m,s}}{\partial \Theta_3} \right|_{\mathbf{x}=\mathbf{x}_k^-} \\ 0 \\ 0 \\ \delta(1 - m) \\ 0 \\ \delta(2 - m) \\ 0 \\ \vdots \\ \delta(M - m) \end{bmatrix}^T \quad (30)$$

where $\delta(\cdot)$ is the Kronecker function. This measurement vector \mathbf{h} is used to test every base station measurement on plausibility by determining a χ^2 value [19], [20]

$$\chi^2 = (\tilde{\rho}_{m,s} - \mathbf{h}\mathbf{x})(\mathbf{h}\mathbf{P}\mathbf{h}^T + \mathbf{R})^{-1}(\tilde{\rho}_{m,s} - \mathbf{h}\mathbf{x}) \quad (31)$$

where \mathbf{P} is the state estimation covariance matrix and \mathbf{R} the measurement variance of the pseudorange $\tilde{\rho}_{m,s}$. In case the χ^2 value exceeds a predefined threshold limit, the pseudorange of this specific base station is excluded of the measurement update. Due to the additional sensor information in the system, the χ^2 test detects any fault LPM measurement conditions with a high probability.

Depending on the selection process in (31), the sigma point update takes place by combining all LPM and sensor unit measurements in one update process in order to yield the most accurate result.

VI. MEASUREMENTS

The sensor fusion procedures derived in this contribution are tested in a real measurement scenario. For this purpose an LPM arrangement was set up in front of the Abatec AG warehouse in Vöcklabruck. The remote controlled buggy in Fig. 6 has been used as sensor platform.

A. Scenario

Twelve LPM base stations are arranged around the field of view at different heights. Due to the complete coverage of the LPM system the GPS measurements are not taken into account.

B. Results

The estimated trajectory of the sensor unit mounted on the buggy for the 2D position solution is plotted in Fig. 7. As it can be seen the trajectory shows an extremely smooth behavior without any loss of high dynamic tracking performance. This smooth behavior is achieved by additionally available sensor information and not by simply dampening the



Fig. 6. Photo of buggy equipped with multiple sensors for enhanced tracking performance.

noise effects of the tracking filter. The comparison between the true and the estimated movement is done by analyzing a synchronized video recording. Even high dynamic maneuvers like abrupt forward-backward movements are properly estimated.

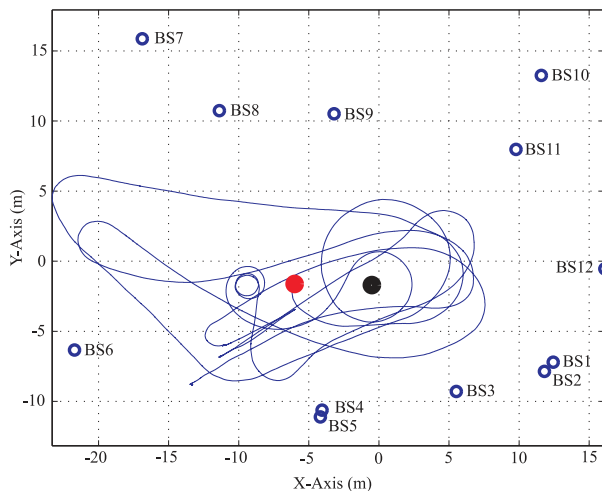


Fig. 7. Estimated trajectory of the buggy equipped with multiple sensors within the LPM field of coverage surrounded by multiple base stations.

VII. CONCLUSION

In this publication multi-sensor data fusion for local positioning applications is discussed. Concordant sensors, combined in a compact design, are used to provide compatible information concerning the movement of the object. Special attention is paid to a robust initialization of an additional Kalman tracking filter for state estimation purposes to avoid potential filter failures.

The derived algorithms for multi-sensor data fusion are tested in a real world measurement scenario. A agile maneuvering buggy, equipped with accelerometers, gyroscopes, a rotary encoder as well as multiple

transponders to gain additional pseudorange measurements, is precisely tracked.

ACKNOWLEDGMENT

This work was funded (in part) by the COMET K2 Center "Austrian Center of Competence in Mechatronics (ACCM)". The COMET program is funded by the Austrian federal government, the federal state Upper Austria and the scientific partners of the ACCM.

APPENDIX

TABLE I
NOMENCLATURE

m	transponder index
M	number of transponders in the system
n	time index n of individual measurements
N_m	number of measurements of transponder m
N	sum of measurements of all transponders
s	base station index s
Θ	parameter vector to estimate
ξ	nonlinear transformed parameter vector
k	IRLS iteration index
	kalman filter time index, respectively
\hat{x}_k^-	<i>a priori</i> state estimate
\hat{x}_k^+	<i>a posteriori</i> state estimate
x, y, v	the vehicle's x, y position and velocity
ψ	heading angle
ω	heading angular velocity
ω^{bias}	gyroscope bias
$w_{m,\text{osc}}$	oscillator drift of transponder m
$v_{m,\text{osc}}$	oscillator drift velocity of transponder m
$C_{\text{bod}}^{\text{nav}}$	direction cosine matrix, body \rightarrow navigation frame
z_p	high of the field of view relative to the BSs
$\mathbf{l}_m^{\text{bod}}$	offset vector of MT m in body coordinates
d	distance from tracking point to rear wheel
R_{Wheel}	wheel radius

REFERENCES

- [1] A. Stelzer, A. Fischer, F. Weinberger, and M. Vossiek, "RF-Sensor for a Local Position Measurement System," in *Proc. 8th NDE Symposium: Nondestructive Detection and Measurement for Homeland Security Conference*, San Diego, CA, USA, March 2–6, 2003, pp. 136–144.
- [2] A. Stelzer, K. Pourvoyeur, and A. Fischer, "Concept and Application of LPM - A Novel 3-D Local Position Measurement System," *Microwave Theory and Techniques, IEEE Transactions on*, vol. 52, no. 12, pp. 2664–2669, 2004.
- [3] M. I. Skolnik, *Introduction to Radar Systems*, 3rd ed. Boston, MA: McGraw-Hill, 2001.
- [4] R. A. Poisel, *Electronic warfare target location methods*. Norwood, MA: Artech House, 2005.
- [5] A. Stelzer, K. Pourvoyeur, A. Fischer, and G. Gassenbauer, "A local position measurement system with integrated telemetry channel," in *Radio and Wireless Symposium, 2006 IEEE*, 2006, pp. 91–94.
- [6] P. Scherz, A. Haderer, K. Pourvoyeur, and A. Stelzer, "Embedded sensor fusion system for unmanned vehicle navigation," in *Mechtronik and Embedded Systems and Applications, 2008. MESA 2008. IEEE/ASME International Conference on*, 2008, pp. 192–197.
- [7] K. Pourvoyeur, A. Stelzer, S. Schuster, and G. Gassenbauer, "Error propagation of GPS in comparison to the local position measurement system LPM," in *Proc. European Conference on Wireless Technology (ECWT)*, Manchester, UK, Sept. 10–12 2006, pp. 335–338.
- [8] S. Bancroft, "An Algebraic Solution of the GPS Equations," *IEEE Transactions on Aerospace and Electronic Systems (AES)*, vol. 21(7), pp. 56–59, Jan. 1985.
- [9] K. Pourvoyeur, A. Stelzer, and G. Gassenbauer, "Position Estimation Techniques for the Local Position Measurement System LPM," in *Proc. Asia Pacific Microwave Conference (APMC) on CD-ROM*, Yokohama, Japan, Dec. 12–15 2006.
- [10] S. M. Kay, *Fundamentals of Signal Processing - Estimation Theory*. Upper Saddle River, NJ: Prentice-Hall, 1993.
- [11] R. C. Aster, B. Borchers, and C. H. Thurber, *Parameter Estimation and Inverse Problems*. Oxford, UK: Elsevier Academic Press, 2005.
- [12] S. Julier and J. Uhlmann, "Unscented filtering and nonlinear estimation," *Proceedings of the IEEE*, vol. 92, no. 3, pp. 401–422, 2004.
- [13] E. Wan and R. V. D. Merwe, "The unscented kalman filter for nonlinear estimation," in *Adaptive Systems for Signal Processing, Communications, and Control Symposium 2000. AS-SPCC. The IEEE 2000*, 2000, pp. 153–158.
- [14] R. Van der Merwe, "Sigma-Point Kalman Filters for Probabilistic Inference in Dynamic State-Space Models," Ph.D. dissertation, OGI School of Science & Engineering at Oregon Health & Science University, Portland, OR., April 2004.
- [15] —, "Sigma-Point Kalman Filters for Nonlinear Estimation and Sensor-Fusion: Applications to Integrated Navigation," in *Proceedings of the AIAA Guidance, Navigation & Control Conference*, Providence, RI, Aug 2004.
- [16] D. Simon, *Optimal State Estimation*. Hoboken, NJ: John Wiley & Sons, Inc., Jan. 2006.
- [17] M. S. Grewal and A. P. Andrews, *Kalman Filtering: Theory and Practice Using Matlab*, 3rd ed. Hoboken, NJ: John Wiley & Sons, Inc., 2008.
- [18] J. Wendel, *Integrierte Navigationssysteme*. Munich, Germany: Oldenbourg Wissenschaftsverlag GmbH, 2007.
- [19] A. Papoulis, *Probability, Random Variables, and Stochastic Processes*, 3rd ed. New York, NY: McGraw-Hill, 1991.
- [20] M. S. Grewal, L. R. Weill, and A. P. Andrews, *Global Positioning Systems, Inertial Navigation, and Integration*. New York, NY: John Wiley & Sons, 2001.